Thesis Title:	**Rational Design of Semiconductors for Efficient Charge Transfer and Light Harvesting for Enhanced Photovoltaic and Sensing Applications**
Name of the Candidate:	Mr. Mohammad Shaad Ansari
Registration Number:	136122015
Thesis Supervisor:	Prof. Mohammad Qureshi
Department:	Chemistry
Institute:	Indian Institute of Technology Guwahati, Assam – 781039, India.

Thesis Overview

Chapter 1: Introduction and Literature Survey

Recent progress in rational design and synthesis of several semiconductors based on their morphologies, accountable for the improved charge transfer and light harvesting ability have been discussed in the present chapter. An overview on photovoltaic technology, basic concepts and working principle of dye-/ semiconductor quantum dot (QD) sensitized solar cells are briefly discussed. This chapter also includes a brief literature survey of current state of art scenario and challenges related to the rational design of semiconductors, utilized for photoanodic segment. Advantages of zinc oxide (ZnO) as a photoanodic material have been discussed over traditionally used titanium dioxide (TiO_2) to get the different morphological structures, to improve the charge carrier dynamics as well as light harvesting of the photoanodic material. With respect to present state of art, templating agents used for tuning the morphology have several drawbacks in terms of the high cost, difficult to remove and environmental unfriendly. Therefore, with low cost and environmentally benign, bio-mass derived templating agents are used for tuning the morphologies of semiconductors. A brief discussion related to the development of chemiresistor device, basic architecture and working principle for gas sensing are also included. This chapter is concluded with a brief literature survey related to ZnO based NH_3 gas sensing.

Chapter 2: Experimental Section

Comprehensive routes for the synthesis and fabrication of materials and basic instrumentation techniques used for material characterization have been discussed in chapter **2**. This chapter also includes photoanode preparation, sensitization and characterization of the photovoltaic devices using the various instrumental techniques/methods. Photovoltaic parameters of devices are characterized using instrumental techniques such as Keithley 2400 (current–voltage characteristics), IQE–200 (incident photon-to-current efficiency, IPCE analyzer) and CHI 680D (electrochemical impedance spectroscopy, EIS measurements). This chapter is concluded with the fabrication of chemiresistor device and sensing assembly, utilized for detection of gas vapors. Sensing studies of chemiresistor device are characterized using Keithley 4200–SCS.

Chapter 3: Morphological Tuning of Photo-booster g–C_3N_4 with Higher Surface Area and Better Charge Transfers for Enhanced Power Conversion Efficiency of Quantum Dot Sensitized Solar Cells

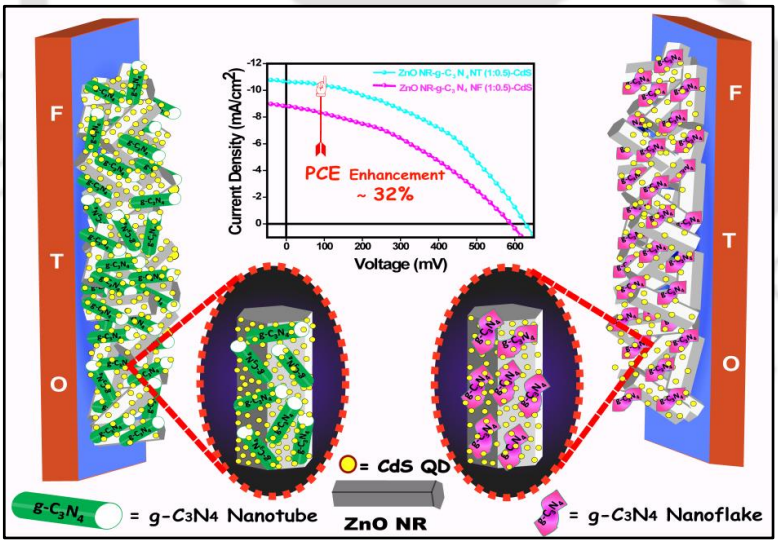

Figure 1. Schematic representation of comparative photovoltaic study of both morphological structures of g–C_3N_4 based solar devices. **[(Carbon 2017, 121, 90–105)]**

In this chapter, photo-booster effect of g-C_3N_4 Nanotubes (g-C_3N_4 NTs) on the photovoltaic properties is investigated using the composites having ZnO Nanorods (NRs) with different composition ratios, sensitized by CdS quantum dots. Enhanced performance is

attributed to the cumulative effects of this composite i.e., (i) a significant decrement of fluorescence intensity in steady state photoluminescence (PL), (ii) faster electron lifetime and good electron injection rate from dynamic PL, and (iii) sufficient loading of sensitizer at photoanodic scaffold for better harvesting of solar energy. An increase of ~ 32 % in power conversion efficiency (PCE, η) is observed in case of g-C_3N_4 NTs based device as compare to g-C_3N_4 Nanoflakes (g-C_3N_4 NFs). Increased PCE value is mainly due to (i) efficient separation and transportation of the photogenerated charge carriers along a one dimensional (1–D) path, resulting in shorter lifetime of charge carriers and (ii) high surface area which provides more active sites for loading of sensitizer particles, results in an improvement of light harvesting ability. Further, electrochemical impedance spectroscopic (EIS) analyses showed an efficient interfacial charge transfer by reducing the recombination processes i.e., the back transferring of photoexcited electron at electrode/electrolyte interface. Figure **1** depicts the Schematic representation of comparative photovoltaic study of both morphological structures of g-C_3N_4 based solar devices with optimized composites ratio. Morphological features of as-synthesized g-C_3N_4 structures and their utilization in photovoltaic study are depicted in the figure **2** and **3** respectively.

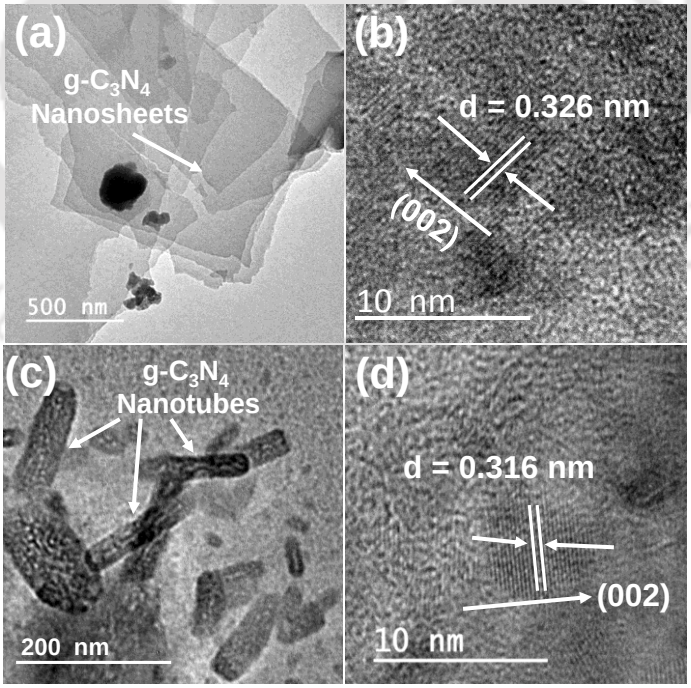

Figure 2. Transmission electron microscopy (TEM) images show the structural features of as-synthesised of g–C_3N_4 NFs [**(a)** and **(b)**] and g–C_3N_4 NFs [**(c)** and **(d)**].

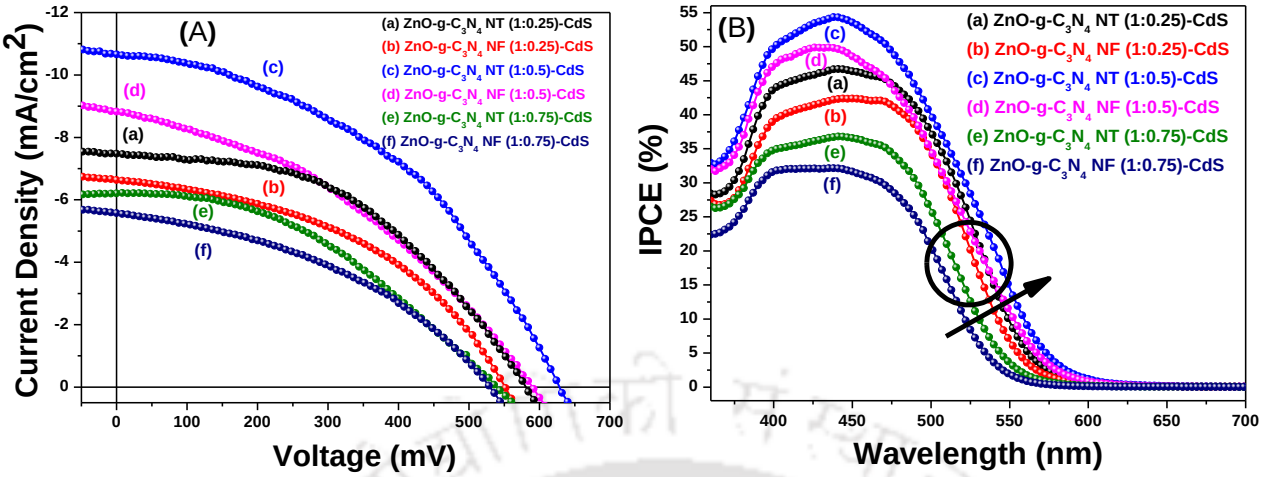

Figure 3. (A) Current density–Voltage (*J*–V) curves for all fabricated photovoltaic devices based on both morphology of g–C_3N_4 with different weight ratios namely: **(a)** ZnO NR–g–C_3N_4 NT (1:0.25)–CdS, **(b)** ZnO NR–g–C_3N_4 NF (1:0.25)–CdS, **(c)** ZnO NR–g–C_3N_4 NT (1:0.5)–CdS, **(d)** ZnO NR–g–C_3N_4 NF (1:0.5)–CdS, **(e)** ZnO NR–g–C_3N_4 NT (1:0.75)–CdS and **(f)** ZnO NR–g–C_3N_4 NF (1:0.75)–CdS. **(B)** Corresponding IPCE plots for the respective devices employing S^{2-}/S_n^{2-} as the redox couple.

Chapter 4: Combined Effect of *In-Situ* Grown p-type $CuSbS_2$ / n-type CdS Coupled with Hierarchical ZnO Nanodisks for Improved Photovoltaic Light Harvesting Efficiency

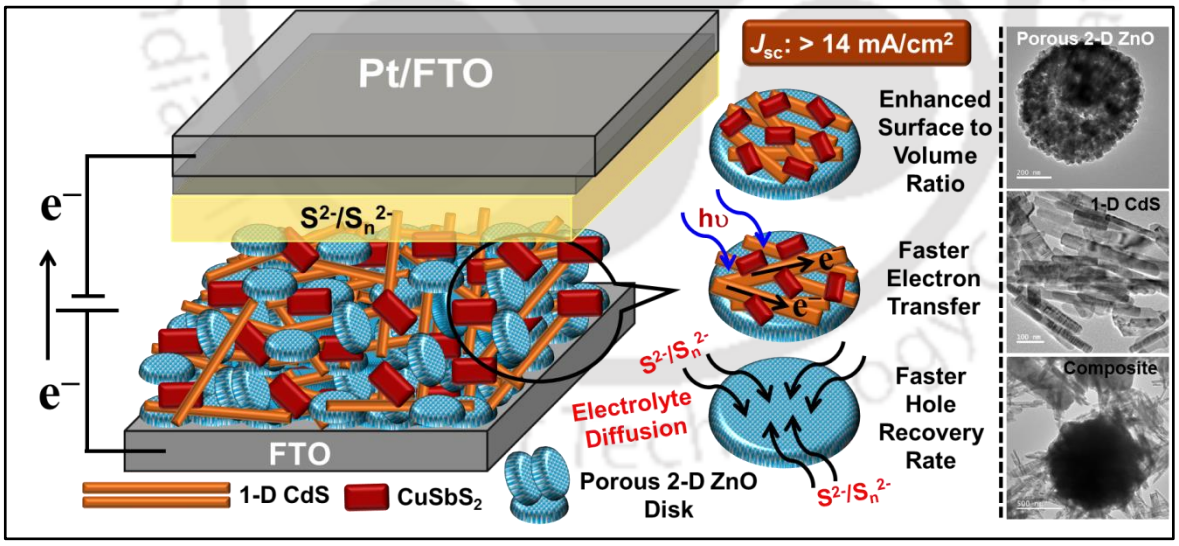

Figure 4. Schematic illustration of various features of photoanodic architecture based on 2–D porous ZnO disk structures, sensitized with 1–D CdS nanowires and $CuSbS_2$ nanobricks. **[(Manuscript under Communication)]**

This chapter demonstrates the synthesis of porous two dimensional (2–D) zinc oxide (ZnO) disk structures, using a biomass derived templating agent i.e., Xanthan gum. This

templating agent is mainly accountable to control the growth kinetics of high energy facets of wurtzite ZnO crystal structure and likely to obtain these disk structures. A comparative photovoltaic study of as-synthesized 2–D porous ZnO structures with respect to 1–D ZnO structures (in absence of xanthan gum) is carried out by co-sensitizing with *in-situ* grown 1–D CdS nanowires array and ternary metal chalcogenide viz. copper antimony sulfide ($CuSbS_2$). Superior photovoltaic performance (~ 45 % enhancement in efficiency) is obtained for CdS-$CuSbS_2$ co-sensitized with 2–D porous ZnO disks as compared to 1–D ZnO structures, owing to improved current density and fill factors. This enrichment is mainly attributed to large exposed surface active sites for optimum loading of light absorbing materials, better light scattering and improved hole recovery rate of sensitizers with the better penetration of redox shuttle. Moreover, crystal phase purity of $CuSbS_2$ (CAS) and p-n junction formed between $CuSbS_2$ and CdS also support the enhanced efficiency by facilitating the electron–hole separation and electron transportation.

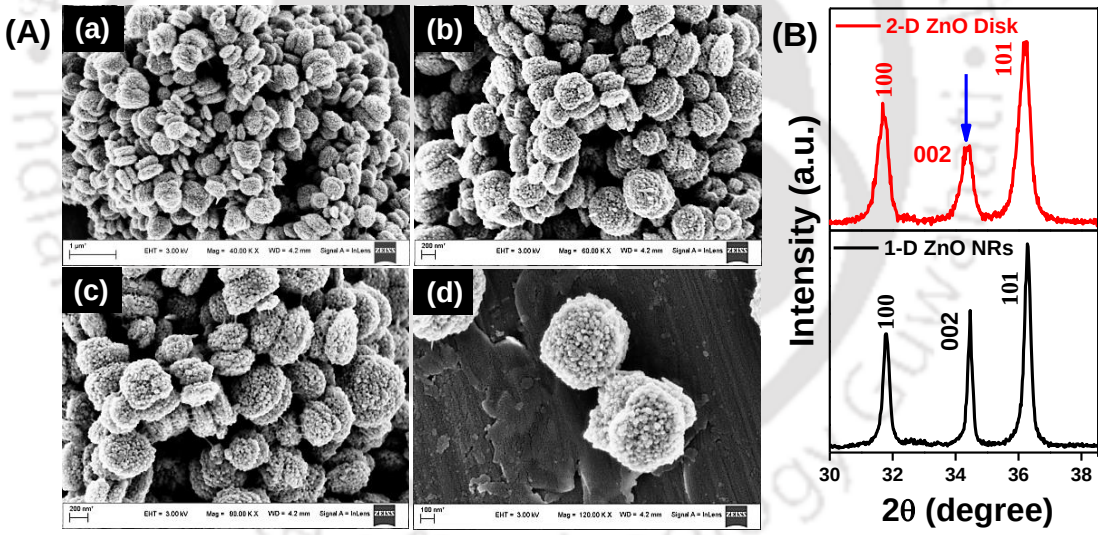

Figure 5. (A) Field emission scanning electron microscopy (FESEM) images show as-synthesized 2−D porous ZnO disk structures [traces **(a−d)**] at different magnifications. **(B)** Powder X-ray diffraction patterns for both ZnO heterostructures, synthesized under different reaction conditions showing intensity variation of the diffraction peaks.

Figure **4** depicts the schematic illustration of various features of photoanodic architecture based on 2–D porous ZnO disk structures, sensitized with *in-situ* 1–D CdS nanowires and $CuSbS_2$ nanobricks. Morphological features with powder x-ray diffraction (PXRD) analysis of as-synthesized 2–D porous ZnO structures and morphology dependent photovoltaic performances based on both ZnO structures are depicted in the figure **5** and **6** respectively.

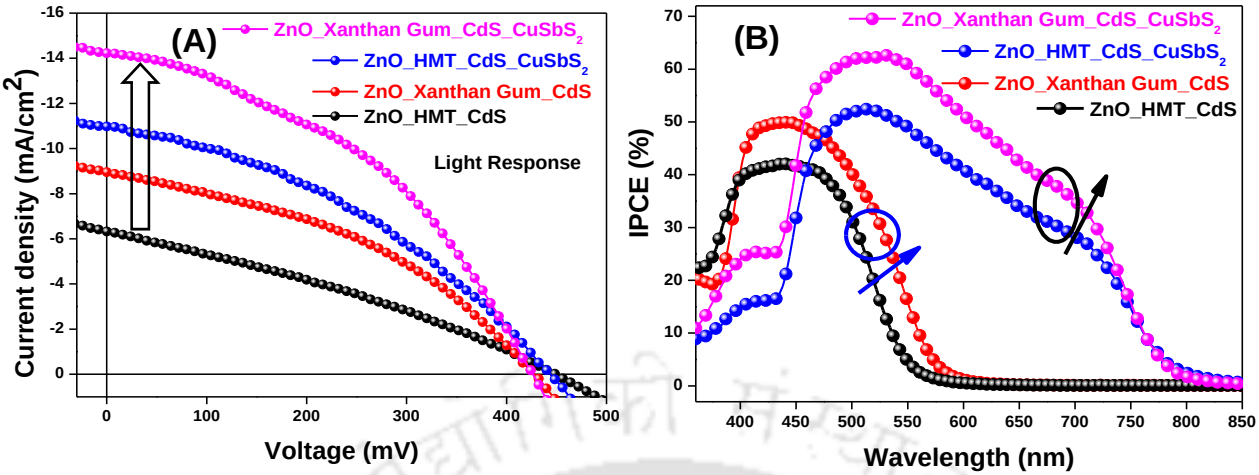

Figure 6. (A) Current density–Voltage (*J*–V) curves for as-fabricated photovoltaic devices based on both morphology of ZnO, sensitized with 1–D CdS and $CuSbS_2$ while **(B)** Corresponding IPCE plots for the respective devices employing S^{2-}/S_n^{2-} as the redox couple.

Chapter 5: Enhanced Photovoltaic Performance using Biomass derived nano 3–D ZnO Hierarchical Superstructures and a D–A type C_S–Symmetric triphenylamine linked bisthiazole

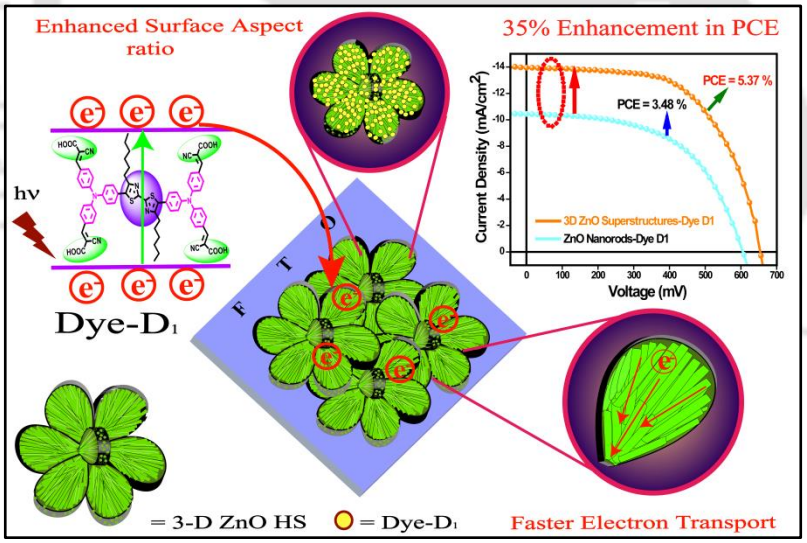

Figure 7. Schematic representation of 3–D hierarchical superstructures based photoanode showing the enhanced surface to volume ratio and fast charge transportation. **[(ACS Omega 2017, 2, 5981–5991; Electrochimica Acta 2018, 259, 262–275)]**

This chapter demonstrates a facile one step biomass assisted hydrothermal route for the controlled synthesis of three dimensional (3–D) Zinc oxide (ZnO) hierarchical superstructures

(HSs), assembled with compacted ZnO nanorods (NRs). Anionic polysaccharide "Polygalacturonic acid" is utilized as a crystal growth modifier for assembling the basic building blocks (ZnO NRs). Probable mechanism for the formation of superstructures through the interaction between the polysaccharide and ZnO growth units is discussed. Photovoltaic properties of as-synthesized 3–D ZnO HSs as compared to its basic structural unit i.e., ZnO NRs are investigated by sensitizing with a bisthiazole linked metal free donor-acceptor dye; **D1**. A substantial enhancement (~ 35%) in efficiency (η) for 3–D ZnO HSs based device (η ≈ 5.37 %) as compare to ZnO NRs (η ≈ 3.48 %) is being observed, mainly due to better charge separation and collection, owing to a superior electron transport ability of compacted building blocks, better light-scattering effect, higher BET surface area for sensitizer loading and efficient electron injection from dye **D1** to the ZnO. Electrochemical impedance spectroscopic (EIS) analysis is carried out to support a slower photogenerated electron–hole recombination rate and better charge transports in the 3–D ZnO HSs based photovoltaic device. Figure **7** shows the schematic representation 3–D hierarchical superstructures based photoanode, exhibiting the enhanced surface to volume ratio and fast charge transportation. Morphological characterizations of as-synthesized 3–D hierarchical ZnO superstructures and photovoltaic performances based on both morphological structures are depicted in the figure **8** and **9** respectively.

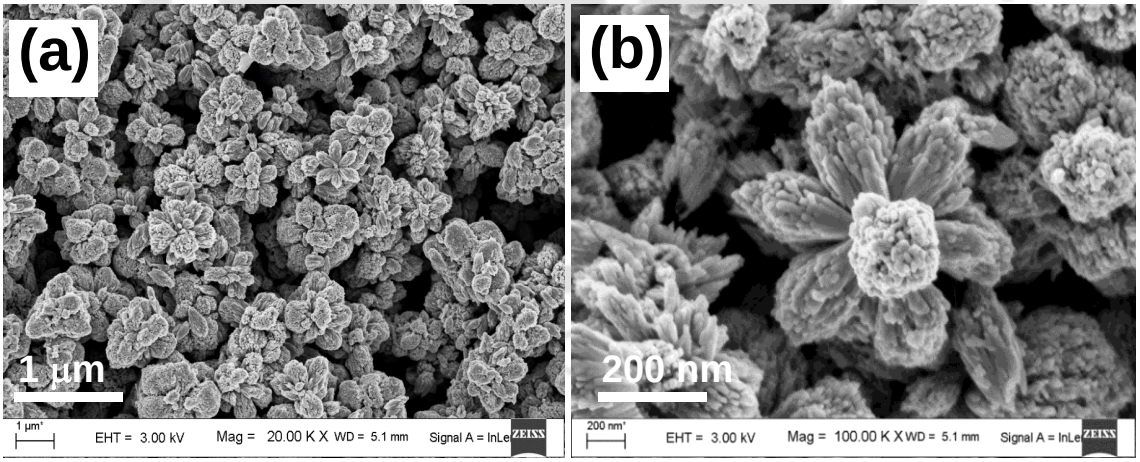

Figure 8. Traces **(a–b)** represent the FESEM images of as-synthesized 3–D ZnO hierarchical superstructures at different magnifications.

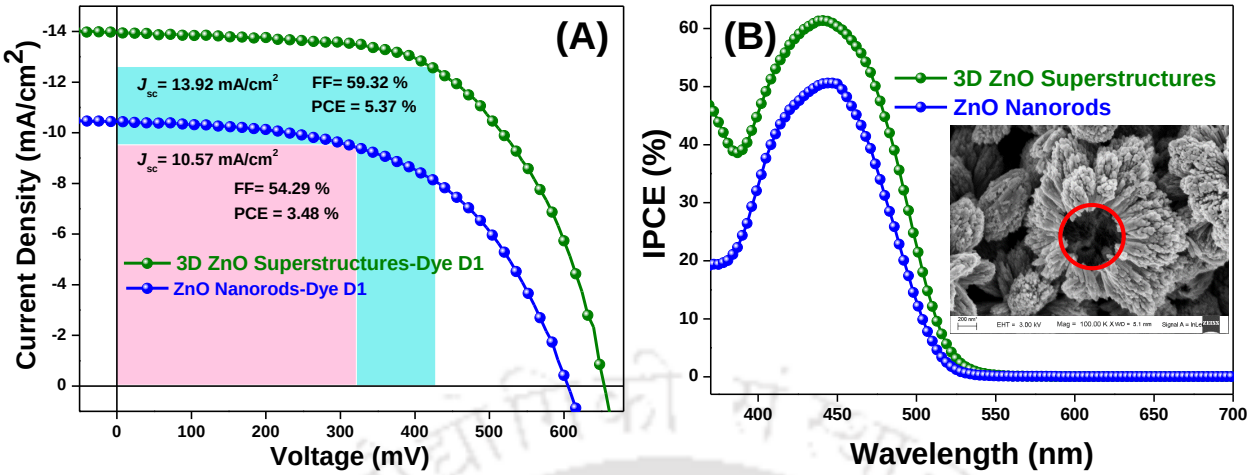

Figure 9. (A) Current density–Voltage (*J*–V) curve for as-fabricated photovoltaic devices based on both ZnO heterostructures. **(B)** Corresponding IPCE plot for the respective devices. Inset shows the porous and hollow nature of ZnO superstructures, helpful for the better infiltration of redox couple and efficient light scattering in the photovoltaic devices.

Chapter 6: Multifunctional Hierarchical 3–D ZnO Superstructures Directly Grown over FTO glass substrates: Enhanced Photovoltaic and Selective Sensing Applications

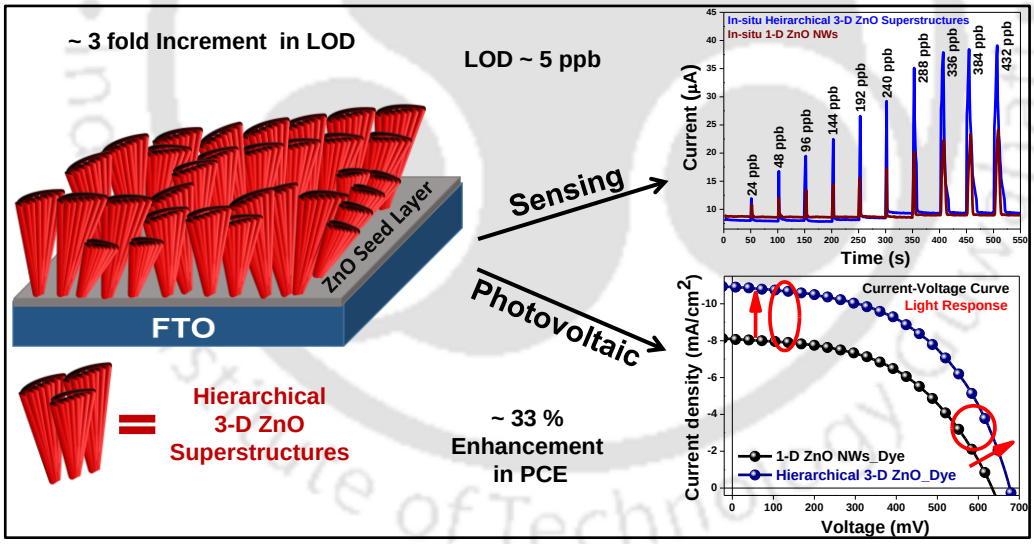

Figure 10. Schematic representation showing 3–D hierarchical superstructures based photoanode and its utilization for Photovoltaic and Gas sensing applications. **[(J. Mater. Chem. A 2018, 6, 15868–15887)]**

This Chapter presents the photovoltaic/sensing device which relies on electron transport; often suffer from the drawback of higher Ohmic contacts between the active materials and its collecting electrode. Designing and developing the chemiresistor device with low ohmic resistance would become more important when the vapor pressure of the compounds yield very

low concentrations of sensing elements. Here, an *in-situ* growth of hierarchical three dimensional Zinc oxide superstructures over conductive glass substrate i.e., fluorine doped tin oxide under controlled hydrothermal route has been reported for low Ohmic contact, thereby an efficient charge injection. An anionic polysaccharide "k-carrageenan" is employed for assisting the hetero epitaxial aggregated growth of 1–D nanocrystals. We have successfully demonstrated the applications of as-characterized multifunctional 3–D ZnO hierarchical structures in photovoltaic and selective chemical vapor sensing. A significant enrichment (~ 33 %) in power conversion efficiency (η) for hierarchical 3–D ZnO superstructures based photovoltaic device as compared to 1–D ZnO nanowires has been observed which is mainly due to the larger surface to volume ratio for sensitizer loading, better light-scattering effect, better charge separation and collection. Two terminal sensor devices have displayed high sensitivity and selectivity for NH_3 vapors with the limit of detection value of ~ 5 parts per billion (ppb) for 3–D ZnO hierarchical superstructures while ~ 17 ppb for 1–D ZnO NWs, which is very less as compared to maximum permissible limit i.e., 25 parts per million (ppm). Selectivity, recyclability, response/recovery time and sensitivity for primary, secondary and tertiary amines are studied for both the chemiresistor devices. Figure 10 illustrates the schematic representation of 3–D hierarchical superstructures based photoanode and its utilization for Photovoltaic and Gas sensing applications. Morphological features of *in-situ* grown 3–D hierarchical ZnO structures and photovoltaic performances are shown in the figure **11** and **12**. Gas sensing studies of both heterostructures of ZnO are depicted in figure **13** while sensing mechanism is illustrated in figure **14**.

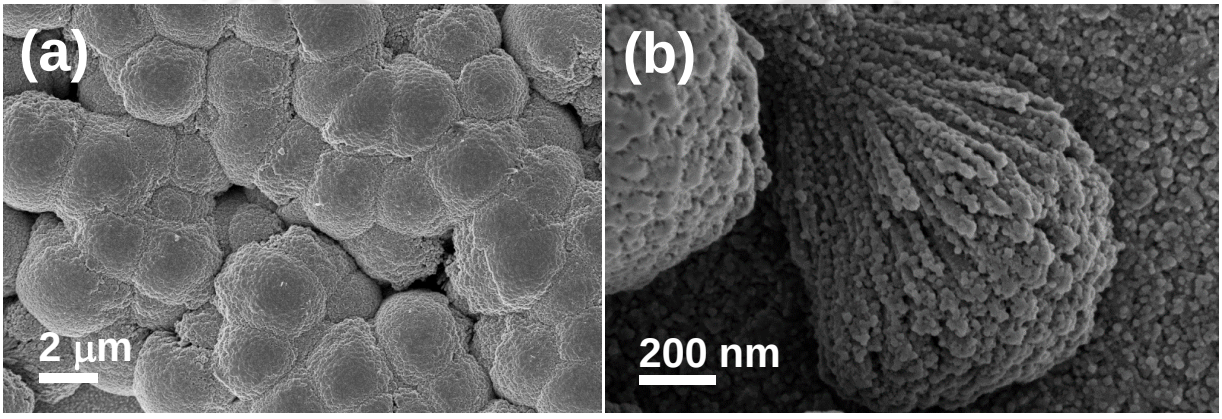

Figure 11. Traces **(a, b)** represent the Field emission scanning electron microscopy (FESEM) images of *in-situ* grown hierarchical 3–D ZnO superstructure of different regions at different magnifications.

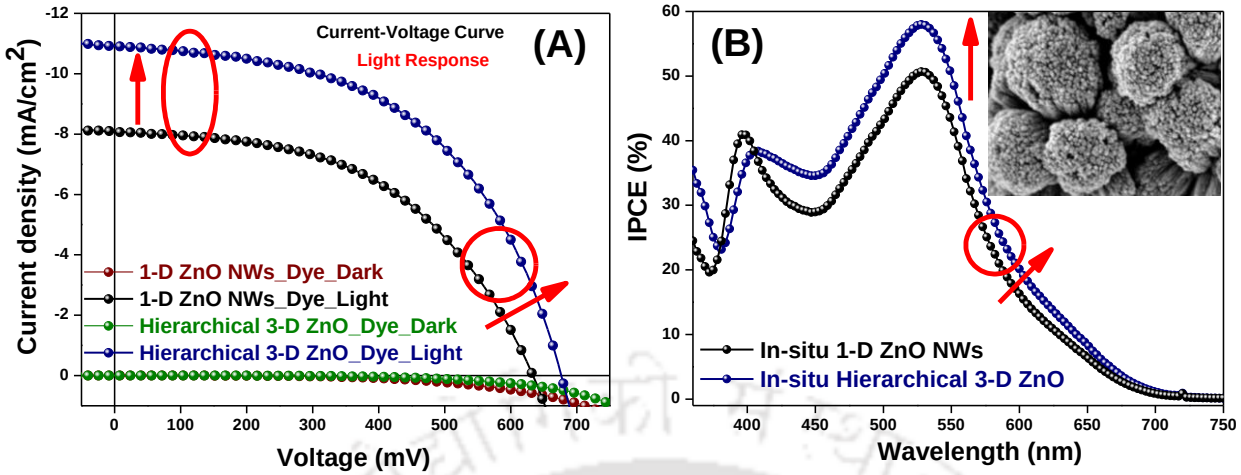

Figure 12. (A) Current density–voltage (*J*–V) curve for both *in-situ* grown ZnO heterostructure-based photovoltaic devices. **(B)** Corresponding IPCE plots for the respective devices. Inset of **(B)** shows the *in-situ* grown hierarchical 3–D ZnO superstructures, helpful for the effective light utilization by providing higher loading sites for sensitizer adsorption.

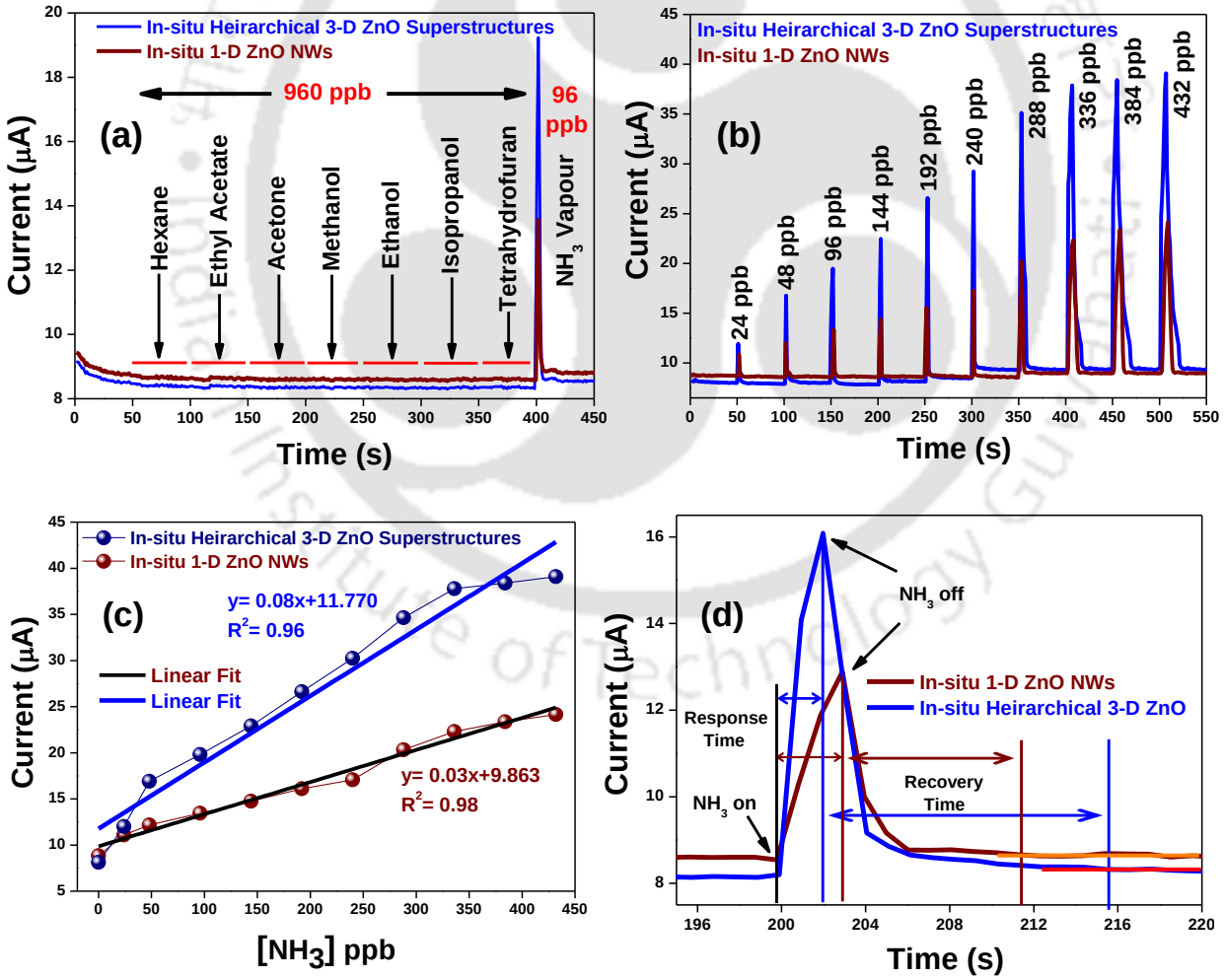

Figure 13. (a) Sensing response of the as-fabricated chemiresistor devices based on both *in-situ* grown ZnO heterostructures for various common organic solvents as well as NH_3 vapors at relative humidity of RH 49 %. **(b)** Sensing response for both devices towards various concentrations of NH_3 vapors (RH 48 %). **(c)** Calibration curve for calculating the limit of detection (LOD) of both chemiresistor devices as a function of NH_3 concentration. **(d)** Response and recovery time of the NH_3 sensing based on both devices (RH 48 %).

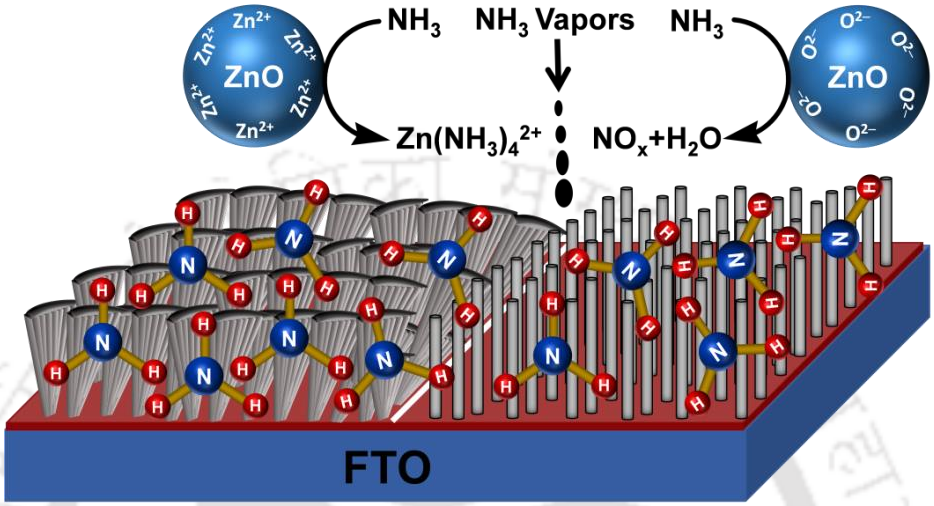

Figure 14. Schematic illustration represents the probable gas sensing mechanism.

Conclusions and Thesis Overview

In conclusion, we have tuned the morphology of UV-Vis light responsive semiconducting materials using different synthetic strategies. Various biomass derived templating agents are explored to modify the structural features of ZnO. These different dimensional ZnO nanostructures are utilized to fabricate the hybrid photoanodes for dye-/ quantum dots sensitized solar cells. Numerous light absorbing materials are employed to construct the photoanodes of highly efficient photovoltaic devices. We have also developed highly selective and sensitive gas sensor device by using different morphological structures of ZnO.